

**A 250-YEAR PERIODICITY IN SOUTHERN HEMISPHERE WESTERLY WINDS
OVER THE LAST 2600 YEARS**

Affiliations: Chris S.M. Turney^{1,2*}, Richard T. Jones³, Christopher Fogwill^{1,2}, Jackie Hatton³, Alan N. Williams^{4,5}, Alan Hogg⁶, Zoë Thomas^{1,2}, Jonathan Palmer^{1,2}, Scott Mooney¹, and Ron W. Reimer⁷

1. School of Biological, Earth and Environmental Sciences, University of New South Wales, Sydney, Australia
2. Climate Change Research Centre, School of Biological, Earth and Environmental Sciences, University of New South Wales, Sydney, Australia
3. Department of Geography, Exeter University, Devon, EX4 4RJ, United Kingdom
4. Fenner School of Environment and Society, The Australian National University, Canberra, ACT 0200, Australia
5. Archaeological & Heritage Management Solutions Pty Ltd, 2/729 Elizabeth Street, Waterloo, NSW 2017, Australia
6. Waikato Radiocarbon Laboratory, University of Waikato, Private Bag 3105, Hamilton, New Zealand
7. School of Geography, Archaeology and Palaeoecology, Queen's University Belfast. Belfast BT7 1NN, U.K.

* E-mail: c.turney@unsw.edu.au

Abstract

Southern Hemisphere westerly airflow has a significant influence on the ocean-atmosphere system of the mid- to high-latitudes with potentially global climate implications. Unfortunately historic observations only extend back to the late nineteenth century, limiting our understanding of multi-decadal to centennial change. Here we present a highly resolved (30-year) record of past westerly wind strength from a Falkland Islands peat sequence spanning the last 2600 years. Situated within the core latitude of Southern Hemisphere westerly airflow, we identify highly variable changes in exotic pollen and charcoal derived from South America which can be used to inform on past westerly air strength. We find a period of high charcoal content between 2000 and 1000 cal. yrs BP, associated with increased burning in Patagonia, most probably as a result of higher temperatures and stronger westerly airflow. Spectral analysis of the charcoal record identifies a pervasive c.250-year periodicity that is coherent with radiocarbon production rates suggesting solar variability has a modulating influence on Southern Hemisphere westerly airflow with important implications for understanding global climate change through the late Holocene.

Keywords: Antarctic Oscillation (AAO); exotic pollen; radiocarbon (^{14}C) dating; solar forcing; Southern Annular Mode (SAM); Southern Hemisphere Westerlies

1 **1. Introduction**

2

3 A major limitation for quantifying the magnitude and impact of change across the
4 Southern Ocean is the relatively short duration or low resolution of ocean-atmosphere
5 records. This is particularly significant with regards to the Southern Hemisphere
6 westerly storm belt, which since the mid-1970s, has undergone a significant
7 intensification and southward shift (Gillett et al., 2008; Messié and Chavez, 2011).

8 One measure of this change in atmospheric circulation is the Southern Annular Mode
9 (SAM), described as the pressure difference between Antarctica (65°S) and the
10 latitude band at around 40°S (Karpechko et al., 2009; Marshall, 2003). Since the mid-
11 1970s, SAM appears to have undergone a positive shift in the troposphere, which has
12 been associated with hemispheric-wide changes in the atmosphere-ocean-ice domains,
13 including precipitation patterns and significant surface and subsurface ocean warming
14 (Cook et al., 2010; Delworth and Zeng, 2014; Domack et al., 2005; Gille, 2008, 2014;
15 Thompson et al., 2011). This trend is projected to continue during the 21st century as
16 a result of both ongoing greenhouse gas emissions and a persistence of the Antarctic
17 ozone hole (Liu and Curry, 2010; Thompson et al., 2011; Yin, 2005), potentially
18 resulting in reduced Southern Ocean uptake of anthropogenic CO₂ (Ito et al., 2010; Le
19 Quéré et al., 2009; Lenton et al., 2013; Marshall, 2003; Marshall and Speer, 2012).

20

21 While no observational records for SAM extend beyond the late nineteenth century
22 (Fogt et al., 2009; Marshall, 2003; Visbeck, 2009), proxy records of past westerly
23 airflow have been generated on annual to centennial timescales through the Holocene
24 (Abram et al., 2014; Björck et al., 2012; Lamy et al., 2010; Lisé-Pronovost et al.,
25 2015; McGlone et al., 2010; Strother et al., 2015; Villalba et al., 2012). Crucially the

26 association between proxies and changes in westerly wind strength and/or latitude is
27 often implied but few provide a direct measure of past airflow or directly test their
28 interpretation through time. One possibility is the identification of exotic airborne
29 particles preserved in sedimentary sequences. Ideally, the peat or lake record should
30 be close enough to the source to have a relatively high input of material (e.g. pollen,
31 charcoal) but not so close that the influx is constant over time. Whilst numerous
32 studies have been undertaken in the Arctic (Fredskild, 1984; Jessen et al., 2011) and
33 the high-latitudes of the Indian and Pacific oceans (McGlone et al., 2000; Scott and
34 van Zinderen Barker, 1985), few have been reported from the south Atlantic. Recent
35 work on a lake core taken from Annekov Island, South Georgia (Strother et al., 2015)
36 demonstrates the considerable potential of this approach but the relatively large
37 distance from the nearest source in South America (Figure 1) (approximately 2100
38 km) limits the delivery of pollen with no charcoal reported.

39

40 Here we report a new high-resolution record of westerly airflow over the past 2600
41 years from the Falkland Islands. The Falkland Islands (52°S) lie within the main
42 latitudinal belt of Southern Hemisphere westerly airflow, 500 to 730 km east of
43 Argentina and 1410 km west of Annekov Island. The close proximity to South
44 America means that these islands receive a relatively high input of particles from the
45 continental mainland (Barrow, 1978; Rose et al., 2012), making them an ideal
46 location to investigate past changes in westerly airflow.

47

48 **2. Methods**

49 The Falkland Islands are a low-lying archipelago in the South Atlantic Ocean,
50 situated in the furious fifties wind belt on the southeast South American

51 continental shelf at 51-52°S, 58-61°W (Figure 1). The Falkland Islands experience
52 a cool temperate but relatively dry oceanic climate, dominated by westerly
53 winds (Otley et al. 2008). Across the year, the temperature ranges from 2.2°C
54 (July) to 9°C (February), with the islands experiencing a relatively low but
55 variable precipitation (typically ranging between 500 and 800 mm/year) lying in
56 the lee of the Andes. Modern climate records show the prevailing wind direction
57 across the Falkland Islands is predominantly from the west with strong winds
58 throughout the year and no significant seasonal variation (Upton and Shaw,
59 2002).

60

61 Climate amelioration following the Last Glacial Maximum led to the
62 establishment of blanket peat across large parts of the islands from 16,500 cal.
63 years BP (Wilson et al., 2002). To investigate past westerly airflow in the late
64 Holocene, an exposed Ericaceous-grass peatland was cored on Canopus Hill,
65 above Port Stanley Airport (51.691°S, 57.785°W, approximately 30 m above sea
66 level) (Figure 1). The one-metre sequence reported here comprises a uniform
67 dark-brown peat from which the uppermost 90 cm was contiguously sampled
68 for pollen, charcoal and comprehensive dating.

69

70 Pollen samples were prepared using standard palynological techniques (Faegri
71 and Iverson, 1975). Volumetric samples were taken every 1 cm along the core
72 and *Lycopodium* spores were added as a 'spike'. The samples were deflocculated
73 with hot 10 % NaOH and then sieved through a 106 µm mesh. The samples then
74 underwent acetolysis, to remove extraneous organic matter before the samples
75 were mounted in silicon oil. Pollen types/palynomorphs were counted at 400 X

76 magnification until a minimum of 300 target grains were identified. The pollen
77 counts were expressed as percentages, with only terrestrial land pollen (TLP)
78 contributing to the final pollen sum. Pollen/palynomorphs were identified using
79 standard pollen keys (Barrow, 1978; Macphail and Cantrill, 2006) and the pollen
80 type slide collection at Exeter University. Past fire activity was assessed using
81 micro-charcoal counts of fragments ($<106\mu\text{m}$) identified on the pollen slides
82 (Whitlock and Larsen, 2001). Counts were undertaken at each level until a fixed
83 total of 50 lycopodium spores were counted and the total expressed as a
84 concentration (fragments per cm^3). More than 99% of charcoal fragments were
85 less than $50\mu\text{m}$ in size, with negligible amounts identified in the $50\text{-}106\mu\text{m}$ and
86 $>106\mu\text{m}$ fractions.

87

88 Terrestrial plant macrofossils (fruits and leaves) were extracted from the peat
89 sequence and given an acid-base-acid (ABA) pretreatment and then combusted
90 and graphitized in the University of Waikato AMS laboratory, with $^{14}\text{C}/^{12}\text{C}$
91 measurement by the University of California at Irvine (UCI) on a NEC compact
92 (1.5SDH) AMS system. The pretreated samples were converted to CO_2 by
93 combustion in sealed pre-baked quartz tubes, containing Cu and Ag wire. The
94 CO_2 was then converted to graphite using H_2 and an Fe catalyst, and loaded into
95 aluminum target holders for measurement at UCI. This was supplemented by
96 ^{137}Cs measurements down the profile to detect the onset of nuclear tests. ^{137}Cs
97 analysis was undertaken following standard techniques with measurements
98 made using an ORTEC high- resolution, low-background coaxial germanium
99 detectors. Detectable measurements were obtained between 8.5 and 9.5 cm and

100 assigned an age of CE 1963, the time of early radionuclide fallout at these
101 latitudes (Hancock et al., 2011).

102

103 The radiocarbon and ^{137}Cs ages were used to develop an age model using a
104 P_sequence deposition model in OxCal 4.2 (Ramsey, 2008) with General
105 Outlier analysis detection (probability=0.05) (Ramsey, 2011). The ^{14}C ages
106 were calibrated against the Southern Hemisphere calibration (SHCal13) dataset .
107 Using Bayes theorem, the algorithms employed sample possible solutions with a
108 probability that is the product of the prior and likelihood probabilities. Taking
109 into account the deposition model and the actual age measurements, the
110 posterior probability densities quantify the most likely age distributions; the
111 outlier option was used to detect ages that fall outside the calibration model for
112 each group, and if necessary, down-weight their contribution to the final age
113 estimates. Modelled ages are reported here as thousands of calendar years BP or
114 cal. BP (Table 1 and Figure 2). The pollen sequence reported here spans the last
115 2600 yrs with an average 30-year resolution (Figure 3).

116

117 To investigate the periodicities preserved in the palaeoenvironmental proxies
118 utilised herein, we undertook Multi-Taper Method (MTM) analysis using a
119 narrowband signal, red noise significance and robust noise background
120 estimation (with a resolution of 2 and 3 tapers) (Thomson, 1982). We also
121 applied single spectrum analysis (SSA), which applies an empirical orthogonal
122 function (EOF) analysis to the autocovariance matrix on the chronologies. Here we
123 undertook a Monte Carlo significance test (95% significance), using a window
124 of 9, a Burg covariance, and 8 components. Both analyses used the software

125 *kSpectra* version 3.4.3 (3.4.5). Wavelet analysis and coherence was undertaken
126 on the 30-year averaged data using the `wt()` and `wtc()` functions respectively
127 in the R package 'Biwavelet' (Gouhier, 2013). The Morlet continuous wavelet
128 transform was applied, and the data were padded with zeros at each end to
129 reduce wraparound effects (Torrence and Webster, 1999). To test the
130 robustness of the obtained periodicities, the Lomb-Scargle algorithm was
131 employed, a spectral decomposition method that computes the spectral
132 properties of time series with irregular sampling intervals (Ruf, 1999), in this
133 instance, the 'raw' charcoal values. This method minimises bias and induced
134 periodicities that may arise from interpolating missing or unevenly spaced data.
135 The technique was undertaken using the `lsp()` function within the 'lomb' R
136 package. Periodicities were extracted from data sets using *Analyseries* (Paillard
137 et al., 1996).

138

139 A measure of solar variability was derived by calculating the ^{14}C production rate
140 using the IntCal13 atmospheric radiocarbon dataset (Reimer et al., 2013) and an
141 ocean-atmosphere box diffusion model (Oeschger et al., 1975); the same as that
142 reported in previous studies (Bond et al., 2001; Turney et al., 2005). The model
143 consists of one box for the atmosphere, one for the ocean mixed layer, 37 boxes
144 for the thermocline, five boxes for the deep ocean and two for the biosphere
145 (short and long residence time) (Stuiver and Braziunas, 1993a). The climate-
146 influenced mixing parameters (air-gas sea exchange, eddy diffusivity, and
147 biospheric uptake and release) were held constant through the run using the
148 same setup as Marine04 (Table 2) (Hughen et al., 2004). The model was
149 parameterized to produce a pre-industrial marine mixed layer ^{14}C of -46.5 ‰

150 and a deep ocean value of -190‰ at CE 1830 for the 2013 marine calibration
151 dataset Marine13 (Reimer et al., 2013).

152

153 **3. Results and Discussion**

154 Only a limited number of Holocene pollen records have been reported from the
155 Falkland Islands (Barrow, 1978). The pollen record in the uppermost 90 cm at
156 Canopus Hill is dominated by *Poaceae* and *Empetrum*, consistent with previous
157 work and today's vegetation (Barrow, 1978; Broughton and McAdam, 2003;
158 Clark et al., 1998). The most significant change in the pollen taxa is a pronounced
159 shift to increased representation of *Asteroideae* (accompanied by a relative
160 decline in *Poaceae*) centered on 47 cm (equivalent to 1100 cal. BP) (Figure 2).

161 Although undifferentiated in the counts, the *Asteroideae* are most likely
162 *Chilliostrichum diffusum*, common on the island across a range of habitats
163 including *Empetrum* heath (Broughton and McAdam, 2003). The shift in the
164 pollen diagram therefore most likely reflects the replacement of upland
165 grasslands by *Empetrum* heath. Highly variable charcoal counts were obtained
166 through the sequence (<106 µm) (Figure 2), with negligible macrocharcoal
167 fragments (>106µm) identified, suggesting there was little or no fire on the site.

168

169 The exotic pollen taxa were expressed as concentration values to explore their
170 changing input onto the site over the last 2600 yrs (Figure 2). Although this data
171 could be re-expressed as a pollen influx, the interpretation of flux data in non-
172 annually laminated sequences can be strongly influenced by the choice of age
173 model and the density of dated points down the core (Davis, 1969; Hicks and
174 Hyvärinen, 1999). Consideration of the radiocarbon and ¹³⁷Cs ages (Table 1)

175 suggests that the depth-age relationship can be described by a linear relationship
176 ($r^2 = 0.98$) below a depth of 18 cm (Figure 3). This means that the pollen (and
177 charcoal) concentration data below this depth are equivalent to influx. In the
178 uppermost section of the core (above 18 cm) a faster rate of sediment
179 accumulation (or less compaction) means that the deposition time is reduced.

180

181 Importantly, the sequence preserves a record of exotic pollen delivery into the
182 site, with *Nothofagus* dominating the input but with trace amounts of *Podocarp*,
183 *Ephedra fragilis* and *Anacardium*-type record (<0.5% total land pollen), all
184 originating from South America. Whilst the low levels of most exotic pollen
185 precludes meaningful interpretation, all samples contain *Nothofagus* (<5% total
186 land pollen), a taxa not known to have grown on the Falkland Islands since the
187 Middle Miocene/Early Pliocene (Macphail and Cantrill, 2006) but has been
188 detected in Lateglacial (Clark et al., 1998) and Holocene (Barrow, 1978)
189 sequences. Producing relatively small pollen grains (20-40 μ m in diameter)
190 (Wang et al., 2000), the nearest source of contemporary *Nothofagus* is South
191 America which extends from 33° in central Chile to 56°S on Tierra del Fuego
192 (Veblen et al., 1996). The youngest arboreal macrofossils of the other exotic taxa
193 are dated to late Tertiary deposits on West Point Island, West Falkland (Birnie
194 and Roberts, 1986).

195

196 Whilst exotic pollen values are relatively low, peaks in *Nothofagus* coincide with
197 increased amounts of charcoal in the Canopus Hill sequence. Importantly,
198 negligible amounts of macro-charcoal (>106 μ m) were identified, suggesting the
199 charcoal has been blown to the site from Patagonia. The aerial delivery of the

200 charcoal to the Falkland Islands is supported by the close correspondence with
201 charcoal in Laguna Guanaco in southwest Patagonia (51°S) (Moreno et al., 2009).
202 Importantly, *Nothofagus* dominates lowland Patagonian vegetation and, in areas
203 away from human activity, was established by 5000 cal. years BP (Iglesias et al.,
204 2014; Kilian and Lamy, 2012), with a stepped expansion in *Nothofagus* at Laguna
205 Guanaco centred on 570 cal. BP (Moreno et al., 2009) and evidence for
206 temporary forest fragmentation during periods of stronger westerly airflow
207 (Moreno et al., 2014). In marked contrast to Patagonia, the Falklands *Nothofagus*
208 pollen record is highly variable and of sufficient concentration to recognize
209 similar changes to those in the charcoal record, with periods of high fire
210 frequency associated with high input of exotic pollen.

211

212 Although charcoal fragments <106µm might reflect fire in the local environment,
213 charcoal of this size can be transported long distances (Clark, 1988). The vast
214 majority of the charcoal fragments <50 µm, comparable in size to exotic
215 *Nothofagus* (20-40µm) and *Podocarpus* (40-50µm in diameter) pollen (Wang et
216 al., 2000; Wilson and Owens, 1999). The close correspondence between the
217 *Nothofagus* pollen record and charcoal fragments in the Canopus Hill sequence
218 on the Falkland Islands strongly suggests similar sources, indicating the higher
219 charcoal counts provides a more robust measure of the westerly airflow. A
220 sustained period of charcoal delivery to the Falkland Islands is observed
221 between 2000 and 1000 cal. BP, with prominent peaks in *Nothofagus* and
222 charcoal recognized at approximately 2400, 2100, 1800-1300, 1000, 550 and
223 250 cal. BP (Figure 2) which we interpret here as stronger westerly wind flow..
224 Our results suggest reports of pre-European human activity on the Falkland

225 Islands as inferred by the presence of charcoal in peat sequences (Buckland and
226 Edwards, 1998) may be premature.

227

228 In contrast to previous work at Annenkov Island which suggested enhanced
229 westerly airflow is associated with wetter conditions (Strother et al., 2015), we
230 observe the reverse. Modern comparisons between the SAM (as a measure of
231 westerly airflow) (Marshall, 2003) and air temperature suggest a positive
232 correlation (Abram et al., 2014). Comparing historic observations of SAM with
233 ERA79 Interim reanalysis (Dee et al., 2011), we observe a highly significant
234 relationship with more positive phases of SAM associated with warmer 2-10
235 metre height air temperatures and wind speeds across much of South America,
236 the Antarctic Peninsula and the Falkland Islands (Figure 4), supporting our
237 interpretation. The contrasting moisture interpretation to that in South Georgia
238 may be a result of the rain shadow effect of the Andes on the Falklands. It should
239 be noted, however, that the reanalysis product used here is only for the period
240 commencing CE 1979 (the satellite era) and that different atmospheric dynamics
241 may have been involved in the delivery of exotic pollen and charcoal to the
242 Falkland Islands on centennial timescales.

243

244 The MTM analysis identifies two different periodicities in the charcoal record
245 (<106 μ m) from Canopus Hill significant above 95%: 242 and 95 yrs, with the
246 former exhibiting a broad multi-decadal peak (Figure 5A). To test whether the
247 MTM spectral peak is robust, we undertook SSA on the sequence chronologies. A
248 Monte Carlo significance test identified a significant periodicity (above 95%) at
249 231 yrs (Figure 5B). Furthermore, the Lomb-Scargle algorithm identified a 268-

250 yr peak (Figure 5C), indicating this periodicity is pervasive through the record
251 regardless of the sampling method, and therefore robust.

252

253 The existence of a 200-250 yr periodicity has been identified in numerous
254 Holocene records globally (Galloway et al., 2013; Poore et al., 2004), including
255 Southern Ocean productivity as recorded in Palmer Deep (Domack et al., 2001;
256 Leventer et al., 1996) and dust deposition over Antarctica (Delmonte et al.,
257 2005). Furthermore, whilst no spectral analysis was undertaken, a series of
258 recurring 200-yr long dry/warm periods have recently been reported from
259 Patagonia over the last three millennia and linked to positive SAM-like
260 conditions (Moreno et al., 2014). The origin of the ~250 yr periodicity may be
261 linked to postulated centennial-scale changes in climate modes of variability
262 including the El Niño-Southern Oscillation (ENSO) (Ault et al., 2013) or Southern
263 Ocean convection (Martin et al., 2013). Importantly, a 200-250 yr periodicity has
264 also been observed in records of atmospheric ^{14}C and ^{10}Be (Adolphi et al., 2014;
265 Steinhilber et al., 2012; Stuiver and Braziunas, 1993b; Turney et al., 2005),
266 suggesting the so-called de Vries solar cycle may play a role (Leventer et al.,
267 1996).

268

269 The detection of solar forcing in palaeo records is highly sensitive to the
270 chronological framework being investigated (Gray et al., 2010). To explore the
271 possible role of solar variability on Southern Hemisphere westerly airflow we
272 first analyzed the modelled production rate of ^{14}C derived from 5-year resolved
273 tree-ring data (Reimer et al., 2013), a cosmogenic radionuclide that is produced
274 in the upper atmosphere (with ^{14}C increasing with reduced solar activity) (Bond

275 et al., 2001; Turney et al., 2005). We resampled the ^{14}C dataset at 30-year
276 resolution to mimic the resolution of the Canopus Hill sequence and compared
277 these to the Total Solar Irradiance (TSI) generated from the polar ice core ^{10}Be
278 which is reported at a 20-30 year resolution (Steinhilber et al., 2009) (Figure 6).
279 Regardless of the dataset used, the same pattern is observed with large
280 amplitude changes in solar irradiance between 2600 and 2300 years ago and
281 from 1300 cal. years BP to present day, but with sustained high irradiance
282 between 2300 and 1300 cal. years BP (Figure 6A, C and E). We find the 5-year
283 resolved IntCal13 dataset produces a periodicity comparable to the Falkland
284 Islands record (225 yrs at 99% confidence; Figure 6A and B). Importantly, when
285 we look at the downscaled records of solar irradiance, the statistical significance
286 decreases in the lower-resolved ^{14}C dataset (230 yrs at 90%; Figure 6C and D)
287 or shifts to a lower frequency in the ^{10}Be record (202 yrs at 99%; Figure 6E and
288 F).

289

290 Our results imply that the central Southern Hemisphere westerlies were
291 particularly strong during 2000 and 1000 cal. BP and/or lay close to the latitude
292 of the Falkland Islands, at least within the South American sector and possibly
293 hemispheric-wide (Turney et al., 2016) (Figure 7). Records of comparable
294 latitude and age from South America are Laguna Guanaco (51°S) (Moreno et al.,
295 2014) and Palm2 (53°S) (Lamy et al., 2010). The Laguna Guanaco record
296 captures a remarkably similar fire history as preserved in the Canopus Hill with
297 a pronounced peak in charcoal over the same period (Figure 7D). In Palm2,
298 accumulation rates of biogenic carbonate provide a proxy for salinity changes in
299 surface fjord waters off the west coast of Chile with lower salinities associated

300 with strong winds and relatively high precipitation, limiting the influence of the
301 open ocean water and reducing biogenic carbonate production. While the
302 dataset from Palm2 does not have the resolution of the other records, a similar
303 trend with pervasive lower salinities (stronger westerly winds) is recorded
304 between 2000 and 1000 cal. yrs BP (Figure 7E). Whilst the change in the trend
305 may be interpreted as reflecting either a change in the latitude and/or strength
306 of the winds, the parallel peaks and troughs in *Nothofagus* and charcoal from
307 Canopus Hill (in contrast to constant *Nothofagus* levels at Laguna Guanaco –
308 (Moreno et al., 2009)) imply the core latitude of the westerly winds has not
309 changed and instead was particularly strong between 2000 and 1000 cal. yrs BP,
310 resulting in increased fire frequency in Patagonia (Holz and Veblen, 2012). This
311 is supported by a study on Patagonian *Fitzroya cupressoides* from 40-42°S (Roig
312 et al., 2001). Whilst a living series spanning 1,229-yrs did not identify a 200-250
313 yr periodicity, a 245 yr cycle was identified in a floating 50,000 yr-old tree ring
314 series of comparable length, consistent with our record suggesting a suppression
315 of this periodicity across a large latitudinal range over the last 1000 years.
316 Importantly, the ~250-yr periodicity identified in the charcoal record varies in
317 amplitude over the last 2600 yrs (Figures 7A-C). A Gaussian filtered curve and
318 wavelet plot shows the ~250 year periodicity is expressed between 2600 and
319 1000 cal. BP, and spans the prominent (sustained) peak in charcoal, with an
320 implied reduction in the expression of the ~250 year periodicity over the last
321 millennium.
322
323 The role changing solar output may have on westerly airflow is not immediately
324 apparent. The strongest inferred winds fall within a millennial-duration period

325 of high solar irradiance (Figure 6). In spite of the relatively muted amplitude of
326 the 225-yr periodicity in the ^{14}C record, wavelet coherence with the charcoal
327 data sampled at 30-year resolution shows coherency centred on 1500 cal. yrs BP
328 (Figure 7H), with the proxy of solar irradiance leading westerly wind strength
329 (arrows up). Furthermore, we observe peaks in solar irradiance leading charcoal
330 on the order of 20-40 years (Figure 7G), suggesting Southern Hemisphere
331 westerly winds may be particularly sensitive to the de Vries cycle during periods
332 of high solar irradiance and less sensitive with reduced solar output. How solar
333 periodicity may influence the strength of Southern Hemisphere westerly airflow
334 is not precisely known. One possibility is that the ~ 250 yr periodicity may
335 change salinity in the North Atlantic (Stuiver and Braziunas, 1993b), driving
336 changes in the Meridional Overturning Circulation that are transmitted globally.
337 However, the existence of the same periodicity in the delivery of dust on to the
338 East Antarctic Ice Sheet (Delmonte et al., 2005) does imply a direct atmospheric
339 link, either through changing sea ice extent or sea surface temperatures, or via
340 the westerlies themselves (Shindell et al., 1999). Recent work has highlight the
341 role of high solar irradiance in increasing troposphere-stratosphere coupling,
342 extending the seasonal length during which stronger Southern Hemisphere
343 westerly winds are experienced at the surface (Kuroda and Yamazaki, 2010),
344 similar to that observed in the Northern Hemisphere (Ineson et al., 2011).
345 Alternatively, recent modelling work suggests insolation changes can lead to
346 increased 'baroclinicity' (Fogwill et al., 2015) or a 'Split Jet' (Chiang et al., 2014),
347 strengthening westerly winds. Further work is required to understand the
348 driving mechanism(s) behind the ~ 250 yr periodicity on global climate.

349

350 **4. Conclusions**

351 Southern Hemisphere westerly airflow is believed to play a significant role in
352 precipitation, sea ice extent, sea surface temperatures and the carbon cycle
353 across the mid to high latitudes. Unfortunately, the observational record only
354 extends back to the late nineteenth century, limiting our understanding of what
355 drives past changes in westerly winds. Although proxies of westerly airflow can
356 provide long-term perspectives on past change, few provide a direct (passive)
357 measure of westerly winds. Exotic pollen and charcoal fragments sourced
358 upwind of sedimentary sequences can potentially provide a valuable insight into
359 past variability. Here we report a new, comprehensively-dated high-resolution
360 pollen record from a peat sequence on the Falkland Islands which lies under the
361 present core of Southern Hemisphere westerly airflow (the so-called 'furious
362 fifties') and spanning the last 2600 years. We observe peaks in taxa from South
363 America (particularly *Nothofagus*) and charcoal fragments (<106µm) that appear
364 to be linked to warm and windy conditions. Spectral analysis identifies a robust
365 ~250-yr periodicity, with evidence of stronger westerly airflow between 2000
366 and 1000 cal. yrs BP. In comparison with other Southern Hemisphere records,
367 the 250-yr periodicity suggests solar forcing plays a role in modulating the
368 strength of the Southern Hemisphere westerlies, something hitherto not
369 recognised, and will form the focus of future research.

370

371

372 **Acknowledgements**

373 CSMT and CF acknowledge the support of the Australian Research Council
374 (FL100100195, FT120100004 and DP130104156). We thank the Falkland

375 Islands Government for permission to undertake sampling on the island (permit
376 number: R07/2011) and Darren Christie for assisting with the fieldwork. Many
377 thanks to Joel Pedro and an anonymous reviewer for their insightful and
378 constructive comments. The data are lodged on the NOAA Paleoclimate Archive.

379

380 **Competing financial interests**

381 The authors declare no competing financial interests.

382

References

- 383
384
385 Abram, N. J., Mulvaney, R., Vimeux, F., Phipps, S. J., Turner, J., and England, M. H.:
386 Evolution of the Southern Annular Mode during the past millennium, *Nature*
387 *Climate Change*, 4, 564-569, 2014.
- 388 Adolphi, F., Muscheler, R., Svensson, A., Aldahan, A., Possnert, G., Beer, J., Sjolte, J.,
389 Bjorck, S., Matthes, K., and Thieblemont, R.: Persistent link between solar activity
390 and Greenland climate during the Last Glacial Maximum, *Nature Geoscience*, 7,
391 662-666, 2014.
- 392 Ault, T. R., Deser, C., Newman, M., and Emile-Geay, J.: Characterizing decadal to
393 centennial variability in the equatorial Pacific during the last millennium,
394 *Geophysical Research Letters*, 40, 3450-3456, 2013.
- 395 Barrow, C.: Postglacial pollen diagrams from south Georgia (sub-Antarctic) and
396 West Falkland island (South Atlantic), *Journal of Biogeography*, 5, 251-274, 1978.
- 397 Birnie, J. F. and Roberts, D. E.: Evidence of Tertiary forest in the Falkland Islands
398 (Ilas Malvinas), *Palaeogeography, Palaeoclimatology, Palaeoecology*, 55, 45-53,
399 1986.
- 400 Björck, S., Rundgren, M., Ljung, K., Unkel, I., and Wallin, Å.: Multi-proxy analyses
401 of a peat bog on Isla de los Estados, easternmost Tierra del Fuego: a unique
402 record of the variable Southern Hemisphere Westerlies since the last
403 deglaciation, *Quaternary Science Reviews*, 42, 1-14, 2012.

404 Bond, G., Kromer, B., Beer, J., Muscheler, R., Evans, M. N., Showers, W., Hoffman,
405 S., Lotti-Bond, R., Hajdas, I., and Bonani, G.: Persistent solar influence on North
406 Atlantic climate during the Holocene, *Science*, 294, 2130-2136, 2001.

407 Bronk Ramsey, C. and Lee, S.: Recent and planned developments of the program
408 OxCal, *Radiocarbon*, 55, 720-730, 2013.

409 Broughton, D. A. and McAdam, J. H.: The current status and distribution of the
410 Falkland Islands pteridophyte flora, *Fern Gazette*, 17, 21-38, 2003.

411 Buckland, P. C. and Edwards, K. J.: Palaeoecological evidence for possible Pre-
412 European settlement in the Falkland Islands, *Journal of Archaeological Science*,
413 25, 599-602, 1998.

414 Chiang, J. C., Lee, S.-Y., Putnam, A. E., and Wang, X.: South Pacific Split Jet, ITCZ
415 shifts, and atmospheric North–South linkages during abrupt climate changes of
416 the last glacial period, *Earth and Planetary Science Letters*, 406, 233-246, 2014.

417 Clark, J. S.: Particle motion and the theory of charcoal analysis: source area,
418 transport, deposition, and sampling, *Quaternary Research*, 30, 67-80, 1988.

419 Clark, R., Huber, U. M., and Wilson, P.: Late Pleistocene sediments and
420 environmental change at Plaza Creek, Falkland Islands, South Atlantic, *Journal of*
421 *Quaternary Science*, 13, 95-105, 1998.

422 Cook, A. J., Poncet, S., Cooper, A. P. R., Herbert, D. J., and Christie, D.: Glacier
423 retreat on South Georgia and implications for the spread of rats, *Antarctic*
424 *Science*, 22, 255-263, 2010.

425 Davis, M. B.: Climatic changes in southern Connecticut recorded by pollen
426 deposition at Rogers Lake, *Ecology*, 50, 409-422, 1969.

427 Dee, D. P., Uppala, S. M., Simmons, A. J., Berrisford, P., Poli, P., Kobayashi, S.,
428 Andrae, U., Balmaseda, M. A., Balsamo, G., Bauer, P., Bechtold, P., Beljaars, A. C. M.,
429 van de Berg, L., Bidlot, J., Bormann, N., Delsol, C., Dragani, R., Fuentes, M., Geer, A.
430 J., Haimberger, L., Healy, S. B., Hersbach, H., Hólm, E. V., Isaksen, L., Kållberg, P.,
431 Köhler, M., Matricardi, M., McNally, A. P., Monge-Sanz, B. M., Morcrette, J. J., Park,
432 B. K., Peubey, C., de Rosnay, P., Tavolato, C., Thépaut, J. N., and Vitart, F.: The ERA-
433 Interim reanalysis: configuration and performance of the data assimilation
434 system, *Quarterly Journal of the Royal Meteorological Society*, 137, 553-597,
435 2011.

436 Delmonte, B., Petit, J., Krinner, G., Maggi, V., Jouzel, J., and Udisti, R.: Ice core
437 evidence for secular variability and 200-year dipolar oscillations in atmospheric
438 circulation over East Antarctica during the Holocene, *Climate Dynamics*, 24, 641-
439 654, 2005.

440 Delworth, T. L. and Zeng, F.: Regional rainfall decline in Australia attributed to
441 anthropogenic greenhouse gases and ozone levels, *Nature Geosci*, 7, 583-587,
442 2014.

443 Domack, E., Duran, D., Leventer, A., Ishman, S., Doane, S., McCallum, S., Amblas, D.,
444 Ring, J., Gilbert, R., and Prentice, M.: Stability of the Larsen B ice shelf on the
445 Antarctic Peninsula during the Holocene epoch, *Nature*, 436, 681-685, 2005.

446 Domack, E., Leventer, A., Dunbar, R., Taylor, F., Brachfeld, S., and Sjunneskog, C.:
447 Chronology of the Palmer Deep site, Antarctic Peninsula: a Holocene

448 palaeoenvironmental reference for the circum-Antarctic, *The Holocene*, 11, 1-9,
449 2001.

450 Faegri, K. and Iverson, J.: *Textbook of pollen analysis*, Blackwell, Oxford, 1975.

451 Fogt, R. L., Perlwitz, J., Monaghan, A. J., Bromwich, D. H., Jones, J. M., and Marshall,
452 G. J.: Historical SAM variability. Part II: Twentieth-Century variability and trends
453 from reconstructions, observations, and the IPCC AR4 models, *Journal of Climate*,
454 22, 5346-5365, 2009.

455 Fogwill, C. J., Turney, C. S. M., Hutchinson, D. K., Taschetto, A. S., and England, M.
456 H.: Obliquity control on Southern Hemisphere climate during the Last Glacial,
457 *Nature Scientific Reports*, 5, 2015.

458 Fredskild, B.: Holocene palaeo-winds and climatic changes in West Greenland as
459 indicated by long-distance transported and local pollen in lake sediments. In:
460 *Climatic Changes on a Yearly to Millennial Basis*, Mörner, N. A. and Karlén, W.
461 (Eds.), Springer Netherlands, Dordrecht, The Netherlands, 1984.

462 Galloway, J. M., Wigston, A., Patterson, R. T., Swindles, G. T., Reinhardt, E., and
463 Roe, H. M.: Climate change and decadal to centennial-scale periodicities recorded
464 in a late Holocene NE Pacific marine record: Examining the role of solar forcing,
465 *Palaeogeography, Palaeoclimatology, Palaeoecology*, 386, 669-689, 2013.

466 Gille, S. T.: Decadal-scale temperature trends in the Southern Hemisphere ocean,
467 *Journal of Climate*, 21, 4749-4765, 2008.

468 Gille, S. T.: Meridional displacement of the Antarctic Circumpolar Current,
469 Philosophical Transactions of the Royal Society A: Mathematical, Physical and
470 Engineering Sciences, 372, doi: 10.1098/rsta.2013.0273, 2014.

471 Gillett, N. P., Stone, D. A., Stott, P. A., Nozawa, T., Karpechko, A. Y., Hegerl, G. C.,
472 Wehner, M. F., and Jones, P. D.: Attribution of polar warming to human influence,
473 Nature Geoscience, 1, 750-754, 2008.

474 Gouhier, T.: biwavelet: Conduct univariate and bivariate wavelet analyses
475 (Version 0.14)
476 . 2013.

477 Gray, L. J., Beer, J., Geller, M., Haigh, J. D., Lockwood, M., Matthes, K., Cubasch, U.,
478 Fleitmann, D., Harrison, G., Hood, L., Luterbacher, J., Meehl, G. A., Shindell, D., van
479 Geel, B., and White, W.: Solar influences on climate, Reviews of Geophysics, 48,
480 n/a-n/a, 2010.

481 Hancock, G. J., Leslie, C., Everett, S. E., Tims, S. G., Brunskill, G. J., and Haese, R.:
482 Plutonium as a chronomarker in Australian and New Zealand sediments: a
483 comparison with ^{137}Cs , Journal of Environmental Radioactivity, 102, 919-929,
484 2011.

485 Hicks, S. and Hyvärinen, H.: Pollen influx values measured in different
486 sedimentary environments and their palaeoecological implications, Grana, 38,
487 228-242, 1999.

488 Hogg, A. G., Hua, Q., Blackwell, P. G., Niu, M., Buck, C. E., Guilderson, T. P., Heaton,
489 T. J., Palmer, J. G., Reimer, P. J., Reimer, R. W., Turney, C. S. M., and Zimmerman, S.

490 R. H.: SHCal13 Southern Hemisphere calibration, 0–50,000 years cal BP,
491 Radiocarbon, 55, 1889-1903, 2013.

492 Holz, A. and Veblen, T. T.: Wildfire activity in rainforests in western Patagonia
493 linked to the Southern Annular Mode, International Journal of Wildland Fire, 21,
494 114-126, 2012.

495 Hua, Q. and Barbetti, M.: Review of tropospheric bomb ^{14}C data for carbon cycle
496 modeling and age calibration purposes, Radiocarbon, 2004.

497 Hughen, K. A., Baillie, M. G., Bard, E., Beck, J. W., Bertrand, C. J., Blackwell, P. G.,
498 Buck, C. E., Burr, G. S., Cutler, K. B., and Damon, P. E.: Marine04 marine
499 radiocarbon age calibration, 0-26 cal kyr BP, Radiocarbon, 46, 1059-1086, 2004.

500 Iglesias, V., Whitlock, C., Markgraf, V., and Bianchi, M. M.: Postglacial history of
501 the Patagonian forest/steppe ecotone (41–43°S), Quaternary Science Reviews,
502 94, 120-135, 2014.

503 Ineson, S., Scaife, A. A., Knight, J. R., Manners, J. C., Dunstone, N. J., Gray, L. J., and
504 Haigh, J. D.: Solar forcing of winter climate variability in the Northern
505 Hemisphere, Nature Geoscience, advance online publication, 2011.

506 Ito, T., Woloszyn, M., and Mazloff, M.: Anthropogenic carbon dioxide transport in
507 the Southern Ocean driven by Ekman flow, Nature, 463, 80-83, 2010.

508 Jessen, C. A., Solignac, S., Nørgaard-Pedersen, N., Mikkelsen, N., Kuijpers, A., and
509 Seidenkrantz, M.-S.: Exotic pollen as an indicator of variable atmospheric
510 circulation over the Labrador Sea region during the mid to late Holocene, Journal
511 of Quaternary Science, 26, 286-296, 2011.

512 Karpechko, A. Y., Gillett, N. P., Marshall, G. J., and Screen, J. A.: Climate impacts of
513 the Southern Annular Mode simulated by the CMIP3 models, *Journal of Climate*,
514 22, 3751-3768, 2009.

515 Kilian, R. and Lamy, F.: A review of Glacial and Holocene paleoclimate records
516 from southernmost Patagonia (49–55°S), *Quaternary Science Reviews*, 53, 1-23,
517 2012.

518 Kuroda, Y. and Yamazaki, K.: Influence of the solar cycle and QBO modulation on
519 the Southern Annular Mode, *Geophysical Research Letters*, 37, n/a-n/a, 2010.

520 Lamy, F., Kilian, R., Arz, H. W., Francois, J.-P., Kaiser, J., Prange, M., and Steinke, T.:
521 Holocene changes in the position and intensity of the southern westerly wind
522 belt, *Nature Geoscience*, 3, 695-699, 2010.

523 Le Quéré, C., Raupach, M. R., Canadell, J. G., and Marland, G. e. a.: Trends in the
524 sources and sinks of carbon dioxide, *Nature Geoscience*, 2009. doi:
525 10.1038/ngeo1689, 2009.

526 Lenton, A., Tilbrook, B., Law, R., Bakker, D., Doney, S., Gruber, N., Hoppema, M.,
527 Ishii, M., Lovenduski, N., and Matear, R.: Sea-air CO₂ fluxes in the Southern Ocean
528 for the period 1990–2009, *Biogeosciences Discussions*, 10, 285-333, 2013.

529 Leventer, A., Domack, E. W., Ishman, S. E., Brachfeld, S., McClennen, C. E., and
530 Manley, P.: Productivity cycles of 200–300 years in the Antarctic Peninsula
531 region: Understanding linkages among the sun, atmosphere, oceans, sea ice, and
532 biota, *Geological Society of America Bulletin*, 108, 1626-1644, 1996.

533 Lisé-Pronovost, A., St-Onge, G., Gogorza, C., Haberzettl, T., Jouve, G., Francus, P.,
534 Ohlendorf, C., Gebhardt, C., Zolitschka, B., and Team, P. S.: Rock-magnetic proxies
535 of wind intensity and dust since 51,200 cal BP from lacustrine sediments of
536 Laguna Potrok Aike, southeastern Patagonia, *Earth and Planetary Science*
537 *Letters*, 411, 72-86, 2015.

538 Liu, J. and Curry, J. A.: Accelerated warming of the Southern Ocean and its
539 impacts on the hydrological cycle and sea ice, *Proceedings of the National*
540 *Academy of Sciences*, 107, 14987-14992, 2010.

541 Macphail, M. and Cantrill, D. J.: Age and implications of the Forest Bed, Falkland
542 Islands, southwest Atlantic Ocean: Evidence from fossil pollen and spores,
543 *Palaeogeography, Palaeoclimatology, Palaeoecology*, 240, 602-629, 2006.

544 Marshall, G.: Trends in the Southern Annular Mode from observations and
545 reanalyses, *Journal of Climate*, 16, 4134-4143, 2003.

546 Marshall, J. and Speer, K.: Closure of the meridional overturning circulation
547 through Southern Ocean upwelling, *Nature Geoscience*, 5, 171-180, 2012.

548 Martin, T., Park, W., and Latif, M.: Multi-centennial variability controlled by
549 Southern Ocean convection in the Kiel Climate Model, *Climate Dynamics*, 40,
550 2005-2022, 2013.

551 McGlone, M., Wilmshurst, J. M., and Wisser, S. K.: Lateglacial and Holocene
552 vegetation and climatic change on Auckland Island, Subantarctic New Zealand,
553 *The Holocene*, 10, 719-728, 2000.

554 McGlone, M. S., Turney, C. S. M., Wilmshurst, J. M., and Pahnke, K.: Divergent
555 trends in land and ocean temperature in the Southern Ocean over the past
556 18,000 years, *Nature Geoscience*, 3, 622-626, 2010.

557 Messié, M. and Chavez, F.: Global modes of sea surface temperature variability in
558 relation to regional climate indices, *Journal of Climate*, 24, 4314-4331, 2011.

559 Moreno, P., François, J., Villa-Martínez, R., and Moy, C.: Millennial-scale variability
560 in Southern Hemisphere westerly wind activity over the last 5000 years in SW
561 Patagonia, *Quaternary Science Reviews*, 28, 25-38, 2009.

562 Moreno, P. I., Vilanova, I., Villa-Martínez, R., Garreaud, R. D., Rojas, M., and De Pol-
563 Holz, R.: Southern Annular Mode-like changes in southwestern Patagonia at
564 centennial timescales over the last three millennia, *Nat Commun*, 5, 2014.

565 Oeschger, H., Siegenthaler, U., Schotterrer, U., and Gugelmann, A.: A box diffusion
566 model to study the carbon dioxide exchange in nature, *Tellus*, 27, 168-192, 1975.

567 Paillard, D., Labeyrie, L., and Yiou, P.: Macintosh program performs time-series
568 analysis, *Eos*, 77, 379, 1996.

569 Poore, R. Z., Quinn, T. M., and Verardo, S.: Century-scale movement of the Atlantic
570 Intertropical Convergence Zone linked to solar variability, *Geophysical Research*
571 *Letters*, 31, L12214, 2004.

572 Ramsey, C. B.: Dealing with outliers and offsets in radiocarbon dating,
573 *Radiocarbon*, 51, 1023-1045, 2011.

574 Ramsey, C. B.: Radiocarbon dating: revolutions in understanding, *Archaeometry*,
575 50, 249-275, 2008.

576 Reimer, P. J., Bard, E., Bayliss, A., Beck, J. W., Blackwell, P. G., Bronk Ramsey, C.,
577 Grootes, P. M., Guilderson, T. P., Hafliðason, H., Hajdas, I., Hatté, C., Heaton, T. J.,
578 Hoffmann, D. L., Hogg, A. G., Hughen, K. A., Kaiser, K. F., Kromer, B., Manning, S.
579 W., Niu, M., Reimer, R. W., Richards, D. A., Scott, E. M., Southon, J. R., Staff, R. A.,
580 Turney, C. S. M., and van der Plicht, J.: IntCal13 and Marine13 radiocarbon age
581 calibration curves 0–50,000 years cal BP, *Radiocarbon*, 55, 1869-1887, 2013.

582 Roig, F. A., Le-Quesne, C., Boninsegna, J. A., Briffa, K. R., Lara, A., Grudd, H., Jones,
583 P. D., and Villagrán, C.: Climate variability 50,000 years ago in mid-latitude Chile
584 as reconstructed from tree rings, *Nature*, 410, 567-570, 2001.

585 Rose, N. L., Jones, V. J., Noon, P. E., Hodgson, D. A., Flower, R. J., and Appleby, P. G.:
586 Long-range transport of pollutants to the Falkland Islands and Antarctica:
587 Evidence from lake sediment fly ash particle records, *Environmental Science &*
588 *Technology*, 46, 9881-9889, 2012.

589 Ruf, T.: The Lomb-Scargle periodogram in biological rhythm research: Analysis of
590 incomplete and unequally spaced time-series, *Biological Rhythm Research* 30,
591 178-201, 1999.

592 Scott, L. and van Zinderen Barker, E. M.: Exotic pollen and long-distance wind
593 dispersal at a Sub-Antarctic island, *Grana*, 24, 45-54, 1985.

594 Shindell, D., Rind, D., Balachandran, N., Lean, J., and Lonergan, P.: Solar cycle
595 variability, ozone and climate, *Science*, 284, 305-308, 1999.

596 Steinhilber, F., Abreu, J. A., Beer, J., Brunner, I., Christl, M., Fischer, H., Heikkilä, U.,
597 Kubik, P. W., Mann, M., McCracken, K. G., Miller, H., Miyahara, H., Oerter, H., and
598 Wilhelms, F.: 9,400 years of cosmic radiation and solar activity from ice cores
599 and tree rings, Proceedings of the National Academy of Sciences of the United
600 States of America, 109, 5967-5971, 2012.

601 Steinhilber, F., Beer, J., and Fröhlich, C.: Total solar irradiance during the
602 Holocene, Geophysical Research Letters, 36, L19704, 2009.

603 Strother, S. L., Salzmann, U., Roberts, S. J., Hodgson, D. A., Woodward, J., Van
604 Nieuwenhuyze, W., Verleyen, E., Vyverman, W., and Moreton, S. G.: Changes in
605 Holocene climate and the intensity of Southern Hemisphere Westerly Winds
606 based on a high-resolution palynological record from sub-Antarctic South
607 Georgia, The Holocene, 25, 263-279, 2015.

608 Stuiver, M. and Braziunas, T. F.: Modeling atmospheric C-14 influences and C-14
609 ages of marine samples to 10,000 BC, Radiocarbon, 35, 137-189, 1993a.

610 Stuiver, M. and Braziunas, T. F.: Sun, ocean, climate and atmospheric $^{14}\text{CO}_2$: an
611 evaluation of causal and spectral relationships, The Holocene, 3, 289-305, 1993b.

612 Thompson, D. W. J., Solomon, S., Kushner, P. J., England, M. H., Grise, K. M., and
613 Karoly, D. J.: Signatures of the Antarctic ozone hole in Southern Hemisphere
614 surface climate change, Nature Geoscience, 4, 741-749, 2011.

615 Thomson, D. J.: Spectrum estimation and harmonic analysis, Proceedings of the
616 IEEE, 70, 1055-1096, 1982.

617 Torrence, C. and Webster, P. J.: Interdecadal changes in the ENSO–Monsoon
618 system, *Journal of Climate*, 12, 2679-2690, 1999.

619 Turney, C. S. M., Baillie, M., Clemens, S., Brown, D., Palmer, J., Pilcher, J., Reimer, P.,
620 and Leuschner, H. H.: Testing solar forcing of pervasive Holocene climate cycles,
621 *Journal of Quaternary Science*, 20, 511-518, 2005.

622 Turney, C. S. M., McGlone, M., Palmer, J., Fogwill, C., Hogg, A., Thomas, Z. A.,
623 Lipson, M., Wilmshurst, J. M., Fenwick, P., Jones, R. T., Hines, B., and Clark, G. F.:
624 Intensification of Southern Hemisphere westerly winds 2000–1000 years ago:
625 evidence from the subantarctic Campbell and Auckland Islands (52–50°S),
626 *Journal of Quaternary Science*, doi: 10.1002/jqs.2828, 2016. doi:
627 10.1002/jqs.2828, 2016.

628 Upton, J. and Shaw, C. J.: An overview of the oceanography and meteorology of
629 the Falkland Islands, *Aquatic Conservation and Freshwater Ecosystems*, 12, 15-
630 25, 2002.

631 van Oldenborgh, G. J. and Burgers, G.: Searching for decadal variations in ENSO
632 precipitation teleconnections, *Geophysical Research Letters*, 32, L15701, doi:
633 15710.11029/12005GL023110, 2005.

634 Veblen, T. T., Hill, R. S., and Read, J.: The ecology and biogeography of *Nothofagus*
635 forests, Yale University Press, 1996.

636 Villalba, R., Lara, A., Masiokas, M. H., Urrutia, R., Luckman, B. H., Marshall, G. J.,
637 Mundo, I. A., Christie, D. A., Cook, E. R., Neukom, R., Allen, K., Fenwick, P.,
638 Boninsegna, J. A., Srur, A. M., Morales, M. S., Araneo, D., Palmer, J. G., Cuq, E.,

639 Aravena, J. C., Holz, A., and LeQuesne, C.: Unusual Southern Hemisphere tree
640 growth patterns induced by changes in the Southern Annular Mode, *Nature*
641 *Geoscience*, 5, 793-798, 2012.

642 Visbeck, M.: A station-based Southern Annular Mode Index from 1884 to 2005,
643 *Journal of Climate*, 22, 940-950, 2009.

644 Wang, P.-L., Pu, F.-T., and Zheng, Z.-H.: Pollen morphology of the genus
645 *Nothofagus* and its taxonomic significance, *Acta Phytotax. Sinica.*, 38, 452-461,
646 2000.

647 Whitlock, C. and Larsen, C.: Charcoal as a fire proxy. In: *Tracking Environmental*
648 *Change using Lake Sediments*, Springer Netherlands, Dordrecht, The
649 Netherlands, 2001.

650 Wilson, P., Clark, R., Birnie, J., and Moore, D. M.: Late Pleistocene and Holocene
651 landscape evolution and environmental change in the Lake Sullivan area,
652 Falkland Islands, South Atlantic, *Quaternary Science Reviews*, 21, 1821-1840,
653 2002.

654 Wilson, V. R. and Owens, J. N.: The reproductive biology of *Totara* (*Podocarpus*
655 *totara*) (Podocarpaceae), *Annals of Botany*, 83, 401-411, 1999.

656 Yin, J. H.: A consistent poleward shift of the storm tracks in simulations of 21st
657 century climate, *Geophysical Research Letters*, 32, 2005.

658
659

Table and Figure Captions

Depth, cm	Wk lab number	Material	%M/ ¹⁴ C BP ± 1 σ	Modelled years BP ± 1σ
8-9	34598	Fruits and leaves	117.0±0.4%M	-16±11
11-12	32994	Fruits and leaves	107.8±0.4%M	-8±2
18-19	37007	Fruits and leaves	107.3±0.3%M	3±31
25-26	35146	Fruits and leaves	95±25	94±66
35-36	37008	Fruits and leaves	647±25	603±29
39-40	33445	Fruits and leaves	761±25	661±28
57-58	32996	Fruits and leaves	1818±25	1672±51
70-71	32350	Fruits and leaves	2235±25	2201±67
97-98	32997	Fruits and leaves	2749±25	2802±32

Table 1: Radiocarbon and modelled calibrated age ranges using SHCal13 (Hogg et al., 2013) and Bomb04SH (Hua and Barbetti, 2004) using the P_sequence and

Outlier analysis option in OxCal 4.2 (Bronk Ramsey and Lee, 2013; Ramsey, 2008).

Parameter	Marine98	Marine04
Air-gas sea exchange	19 moles/m ² /yr	18.8 moles/m ² /yr
Eddy diffusivity	4000 m ² /yr	4220 m ² /yr
Pre-industrial atmospheric [CO ₂]	280 ppm	270 ppm
Initial atmospheric $\Delta^{14}\text{C}$	90‰	100‰

Table 2: Box diffusion model parameters for Marine98 (Bond et al., 2001; Turney et al., 2005) versus Marine04 (Hughen et al., 2004).

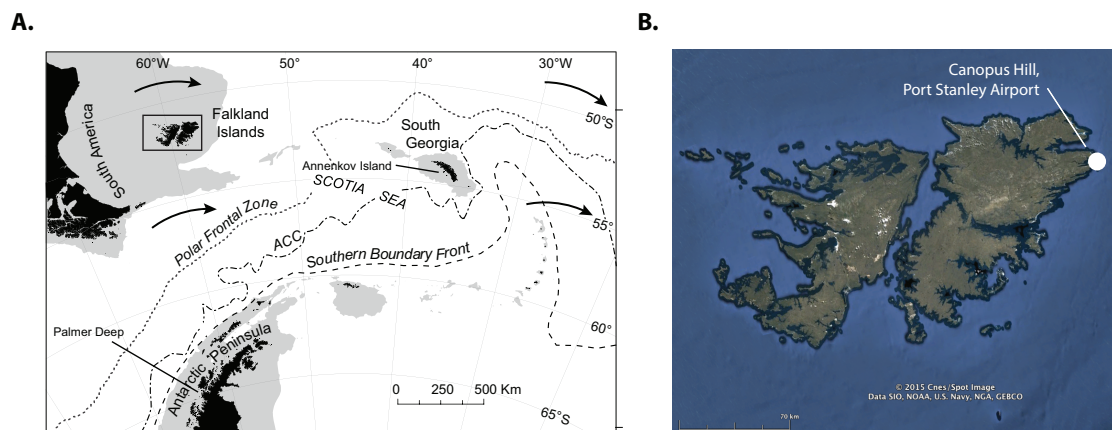


Figure 1: Location of the Falkland Islands in the South Atlantic Ocean with mean locations of the Polar and Southern Boundary fronts (dashed lines), the continental shelf (grey areas) and prevailing westerly airflow (solid arrows) (Panel A); and Canopus Hill, Port Stanley Airport, in the east Falkland Islands (Panel B). Panel ‘A’ was modified from (Strother et al., 2015) and ‘B’ was obtained from Google Earth.

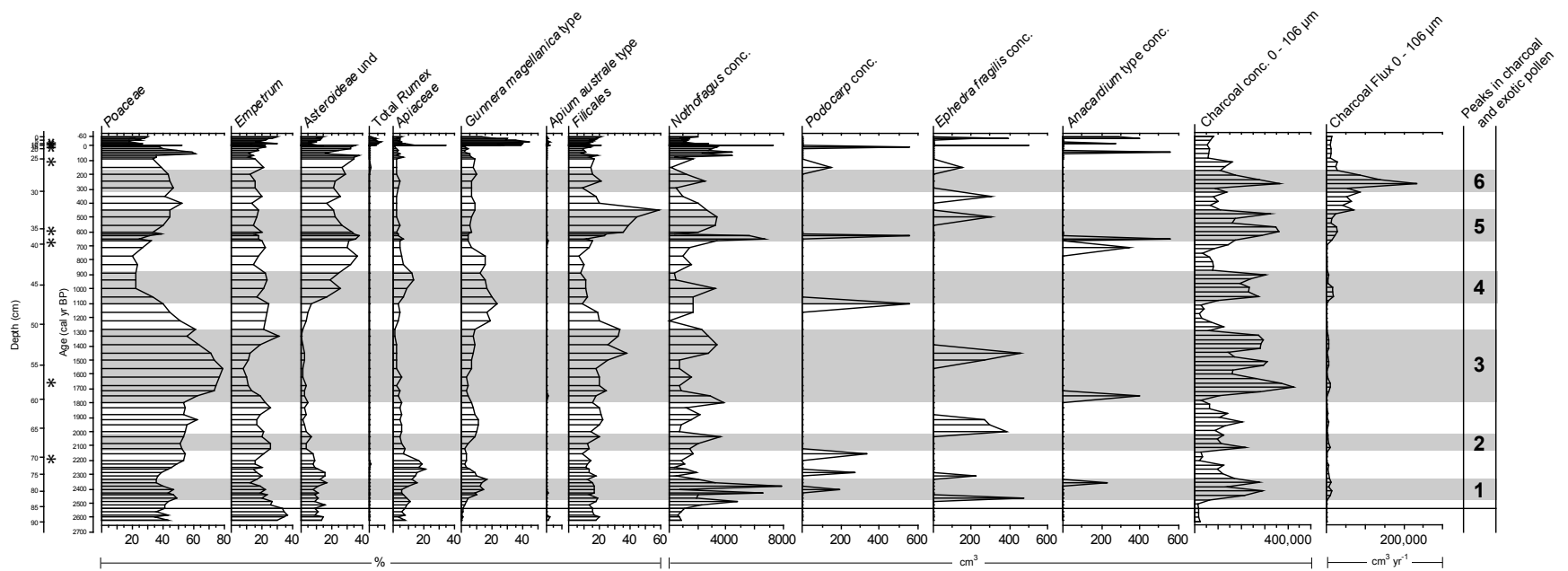


Figure 2: Pollen diagram from Canopus Hill, Port Stanley Airport, plotted against depth and calendar age. The location of ^{137}Cs and ^{14}C ages are marked by asterisk.

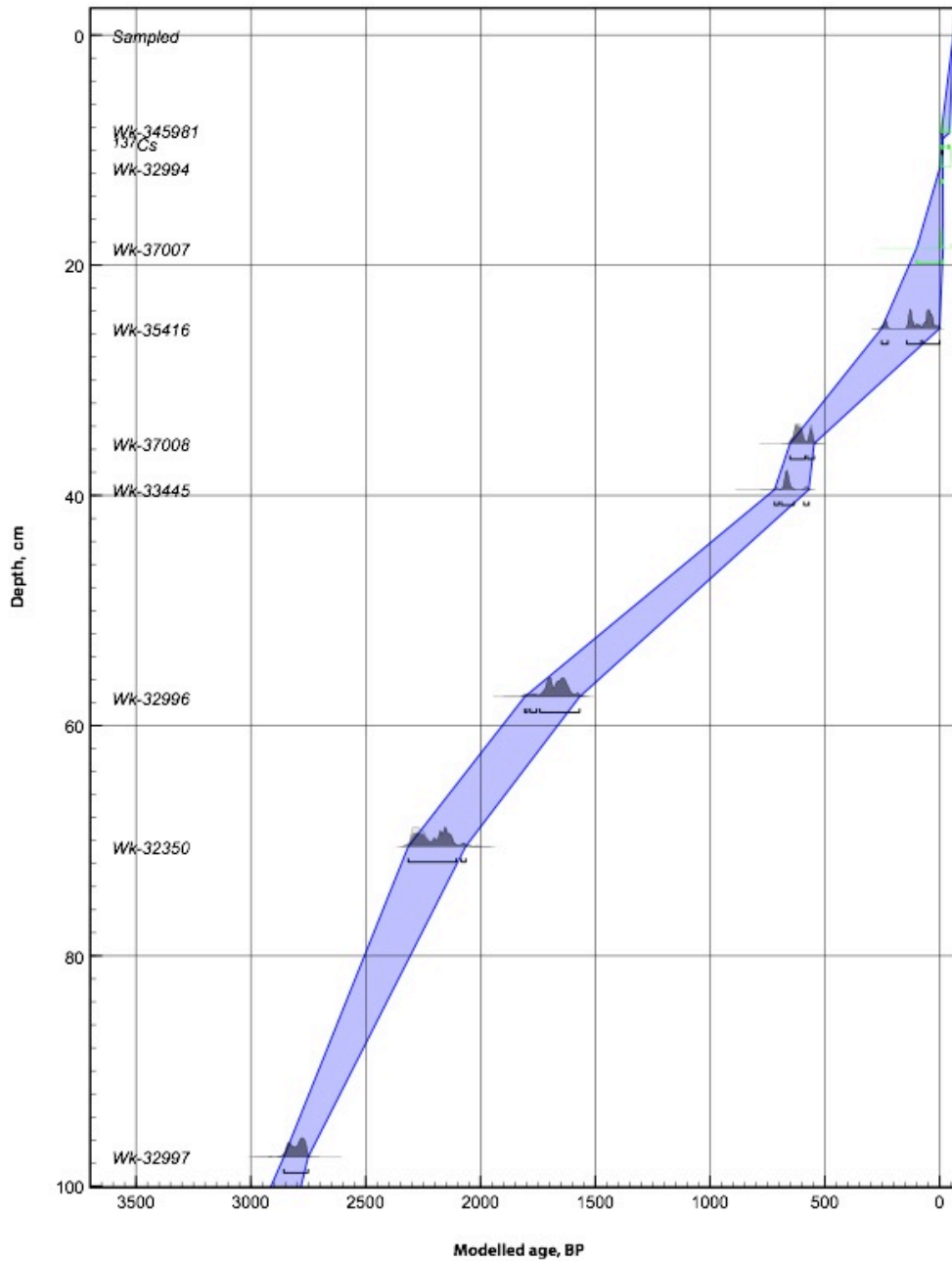


Figure 3: Age-depth plot for Canopus Hill, Port Stanley Airport, with 1σ age range (blue envelope) and probability distributions.

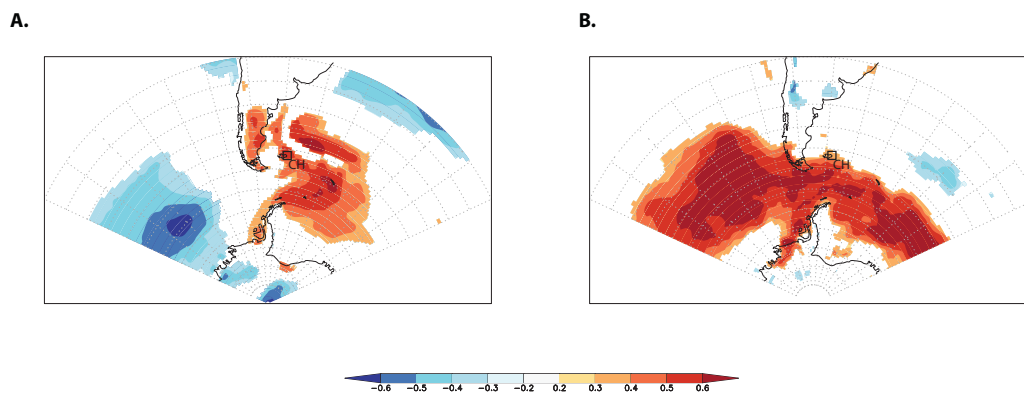
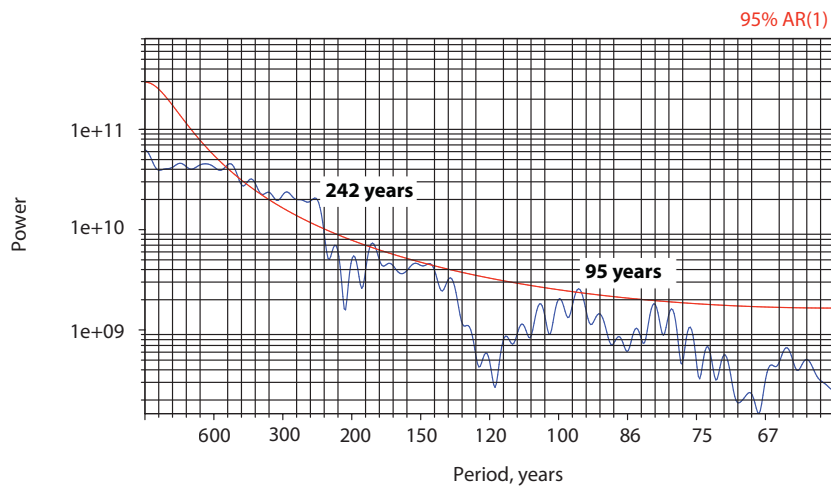
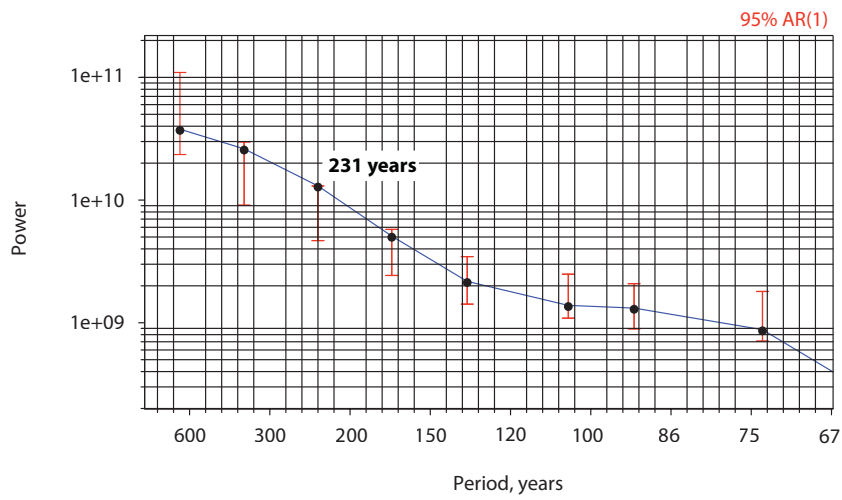


Figure 4: Correlation of relationship between the hemispherically-averaged Southern Annular Mode (SAM) index (Marshall, 2003) with 2-10 metre air temperature (Panel A.) and wind strength (Panel B.) in the ERA-79 Interim reanalysis (Dee et al., 2011) (July-June, 1979-2013). Location of Canopus Hill, (CH), Falkland Islands, shown. Analyses were made with KNMI Climate Explorer (van Oldenborgh and Burgers, 2005).

A.



B.



C.

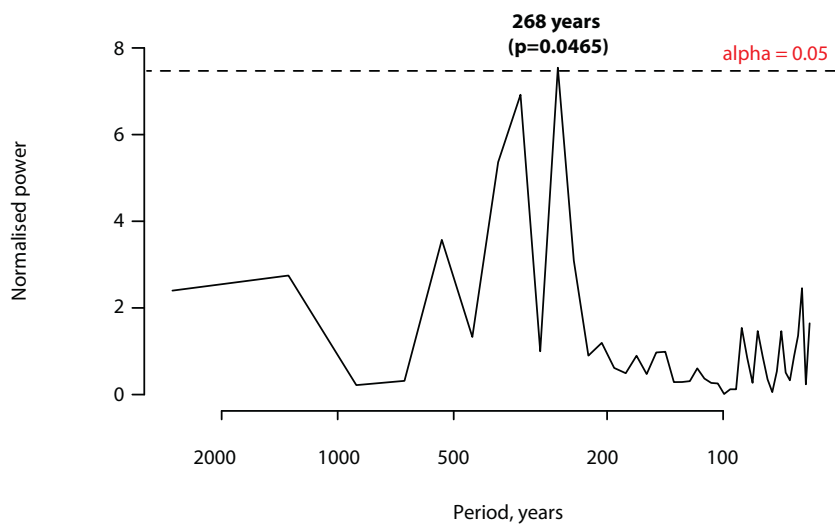


Figure 5: Multi-Taper Method (MTM) (Panel A.), Monte-Carlo Single Spectrum Analysis (SSA) analyses (Panel B.) and Lomb-Scargle analysis (Panel C.) of charcoal from the Canopus Hill sequence. Error bars denote 95% confidence.

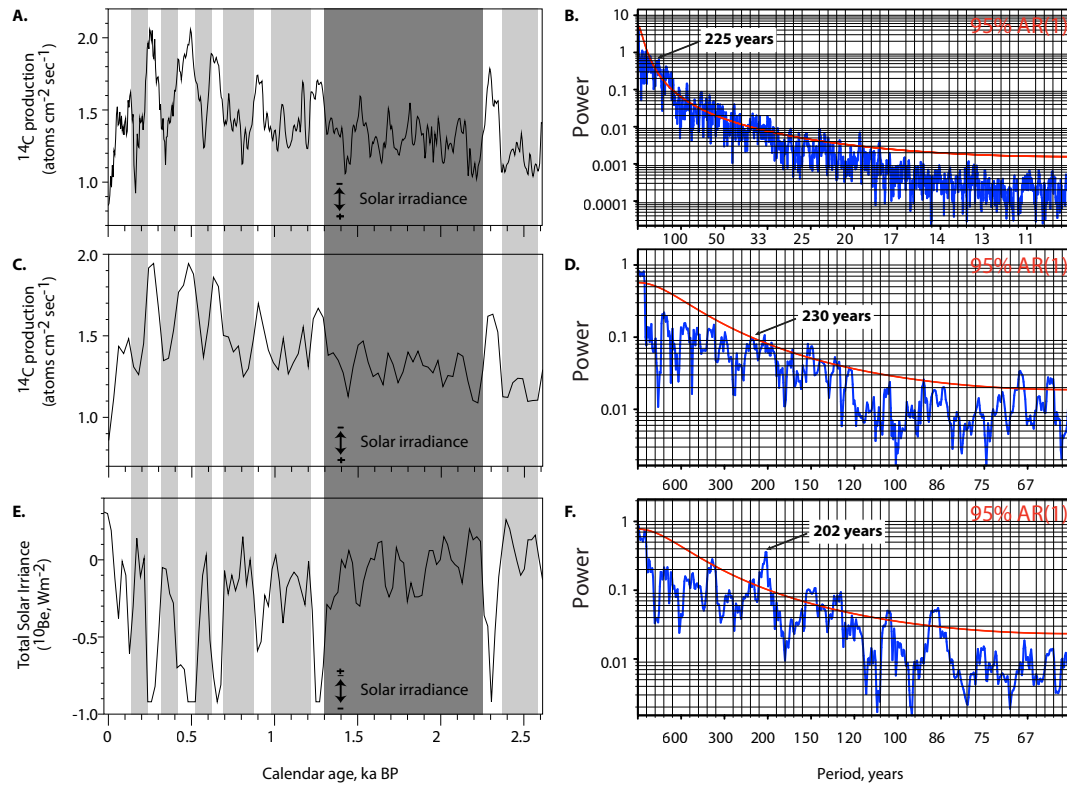


Figure 6: Changes in solar output and Multi-Taper Method (MTM) analysis of reconstructed radiocarbon (^{14}C) production rate (5-yr resolution; this study) (Bond et al., 2001; Turney et al., 2005) (Panels A. and B), ^{14}C production rate (resampled at 30 years) (Panels C. and D.) and Total Solar Irradiance (based on polar ice ^{10}Be) (resampled at 30-yrs) (Panels E. and F.) (Steinhilber et al., 2009) for the full length of each record. The dark gray column defines a millennial-duration period of sustained high solar irradiance in all records; the light gray columns define temporary (centennial-duration) periods of high irradiance. The periodicities that fall within the reported range of the de Vries cycle are identified in the MTM panels (200-230-yrs).

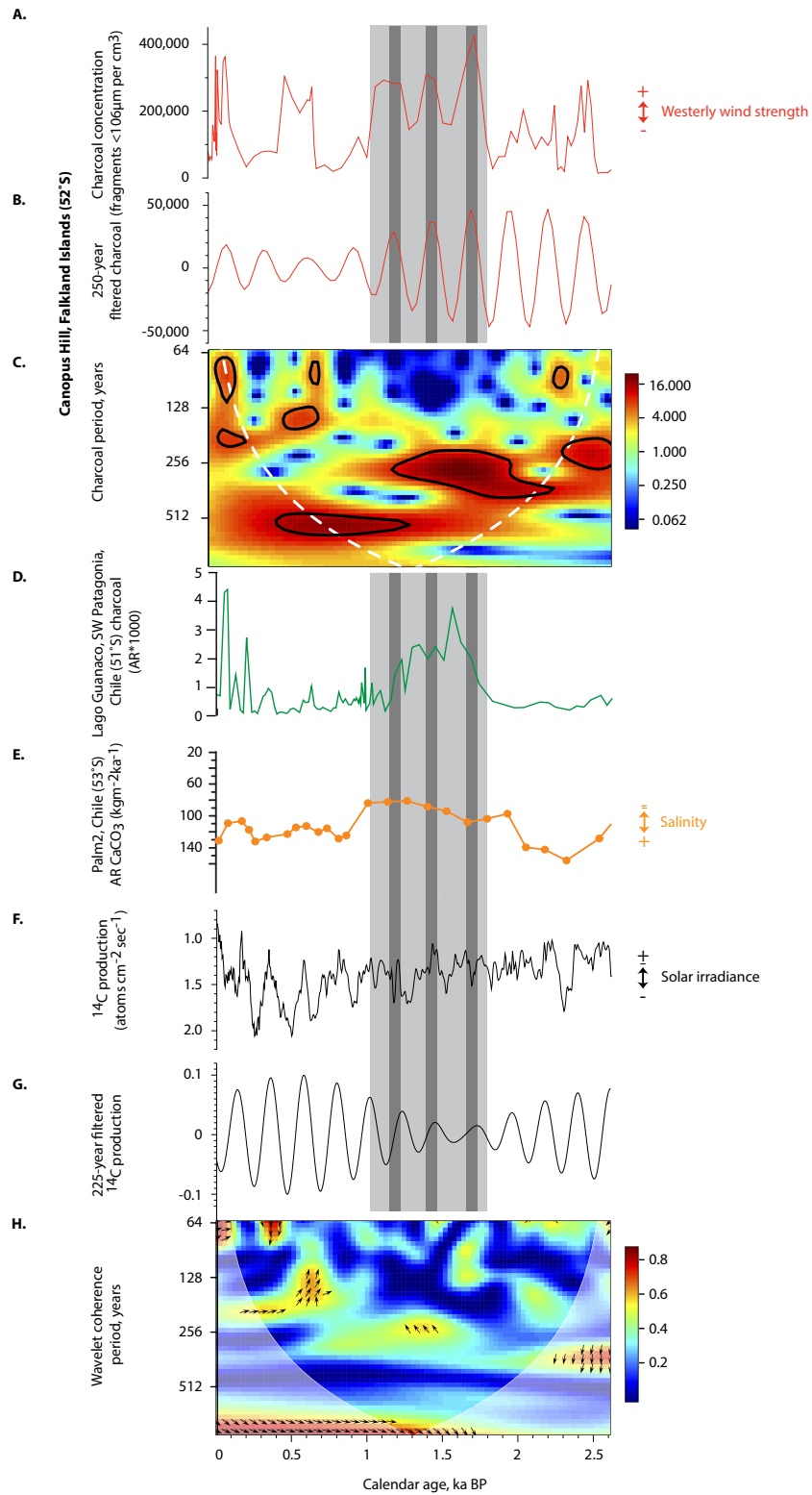


Figure 7: Charcoal concentration (<106µm) (Panel A.), Gaussian-filtered charcoal in the 250-year band (250±25 yr⁻¹) (Panel B.) and wavelet analysis of charcoal concentration (Panel C.) from Canopus Hill, Port Stanley Airport (52°S).

Solid black line in wavelet denotes 95% confidence in periodicity; white dashed line denotes cone of influence. Panel D. shows charcoal concentration data from Laguna Guanaco, Chile (51°S) (Moreno et al., 2009) and Panel E. the biogenic carbonate accumulation rate (AR) from Palm2, Chile (53°S) . Reconstructed ^{14}C production and Gaussian-filtered ^{14}C in the 225-year band ($225 \pm 22.5 \text{ yr}^{-1}$) are plotted in Panels F and G. Wavelet coherence between the 30-year sampled charcoal and ^{14}C production (Panel H); white dashed line denotes cone of influence; arrows pointing up indicate ^{14}C production (solar) leads Falkland Islands charcoal (proxy of Southern Hemisphere westerly strength). The dark grey columns define peaks in charcoal 250-yr periodicity lagging minima in ^{14}C production rate (high solar irradiance); the light grey area describes the period of pervasively stronger winds across the South Atlantic 2000 to 1000 cal. BP.